DOE/NASA/10350-34
NASA TM-82930



# Catalytic Combustion of Actual Low and Medium Heating Value Gases


Daniel L. Bulzan
National Aeronautics and Space Administration
Lewis Research Center

Work performed for
**U.S. DEPARTMENT OF ENERGY**
**Fossil Energy**
**Office of Coal Utilization and Extraction**

Prepared for
1982 Joint Power Generation Conference sponsored by the
American Society of Mechanical Engineers
Denver, Colorado, October 17-21, 1982

# CATALYTIC COMBUSTION OF ACTUAL LOW AND MEDIUM HEATING VALUE GASES

by Daniel L. Bulzan

National Aeronautics and Space Administration
Lewis Research Center
Cleveland, Ohio

E-1326

## INTRODUCTION

Lewis Research Center is currently evaluating catalytic combustion as part of the Critical Research and Advanced Technology Support Project sponsored by the D.O.E. Office of Fossil Energy, Division of Coal Utilization. Catalytic combustion has been shown to be capable of high combustion efficiency and low thermal $NO_x$ emissions when operated on fuels which contain negligible amounts of fuel-bound nitrogen (1,2). Catalytic combustion of residual fuels has also been reported in the literature (3 to 5). Premixing and prevaporizing the residual fuels was found to be a problem and a major drawback for their use as catalytic combustor fuels.

Because of the current interest in increasing the use of coal as an energy source, coal-derived fuels may become important fuel sources for stationary gas turbines. Catalytic combustion of coal-derived liquids was reported (6,7). High combustion efficiencies were reported. However, conversion of fuel-based nitrogen to $NO_x$ was also fairly high. Conversion rates ranged from about 50 to 100 percent. Since the coal-derived liquids contained up to 1 percent nitrogen by weight, $NO_x$ emissions were consequently very high. Coal gasification is an attractive method of utilizing coal without the environmental problems usually associated with the use of coal. Coal gasification can provide a fuel gas which, although lower in heating value than a conventional gaseous fuel such as natural gas, can be relatively free of contaminants such as sulfur and ammonia. The use of a gaseous fuel can also simplify the fuel preparation system required for a catalytic combustor compared to using a liquid fuel.

Catalytic combustion of simulated low- and medium-heating-value gas has been reported in (8,9). A 2.5-cm-diameter catalytic reactor was evaluated using simulated low, 4.5 to 6.7 $MJ/m^3$ (120 to 180 Btu/scf), and medium, 7.5 to 12 $MJ/m^3$ (200 to 320 Btu/scf), heating-value gases at pressures up to $4x10^5$ Pa. Combustion efficiencies greater than 99 percent were measured. Flashback into the premixing zone upstream of the catalytic reactor was reported, however, which required the use of a flashback arrestor upstream of the catalytic reactor. The present paper presents a summary of the more important results obtained from the experimental evaluation of two catalytic reactors using actual coal-derived low- and medium-heating-value gases at conditions representative of stationary gas turbines (10,11). NASA Lewis provided two contractors with essentially identical test hardware to perform the testing. A fluidized bed gasifier, operated by Westinghouse at Waltz Mill, Pennsylvania, was used to produce both low, 5.96 $MJ/m^3$ (160 Btu/scf), and medium, 9.7 $MJ/m^3$, (260 Btu/scf), heating value gas. A fixed-bed gasifier with a complete product gas stream cleanup system, operated by General Electric at Schenectady, New York, was used to produce low, 3.7 $MJ/m^3$ (98 Btu/scf), heating-value gas. Testing was performed in 12 cm inside diameter test rigs at inlet fuel-air mixture temperatures from 500 to 700 K, reference velocities of 10 to 30 m/s, pressures from $5x10^5$ to $15x10^5$ Pa, and adiabatic reaction temperatures from about 1100 to 1450 K. Temperatures, catalytic reactor and fuel injector pressure drop, and emissions of CO, $CO_2$, unburned hydrocarbons, $NO_x$, and $O_2$ were measured.

## EXPERIMENTAL DETAILS

### Test Rig

A schematic drawing of the test rigs is shown in Fig. 1. The test hardware and test rigs were essentially identical for both contractors. Inlet air was indirectly preheated and entered the test

section as shown in Fig. 1. Inlet air temperatures were measured at a plane just upstream of the fuel injector. The test hardware was constructed of 15.24 cm diameter stainless steel pipe which was internally insulated with T30R fiberfrax tube insulation to provide a flow diameter of 12 cm. The fuel injector was composed of two sections mounted in flanges which were bolted together to form the complete unit. One flange contained the fuel tubes. The second contained the fuel injector base into which diffuser passages were machined. The fuel injector is shown in Figs. 2(a) to (d). Schematic drawings of the fuel injector base showing the diffuser passage arrangement and associated dimensions are shown in Figs. 2(a) and (b). A photograph of the fuel injector base mounted in its flange is shown in Fig. 2(c). A photograph of the fuel injector tubes mounted in their flange is shown in Fig. 2(d). Coal-derived gas was injected through 19, 30.5-cm-long tubes into the center of each of the 19 diffuser passages. For the Westinghouse fluidized-bed gasifier, the fuel tubes had a 0.46cm inside diameter and a wall thickness of 0.09 cm. For the General Electric fixed-bed gasifier, the fuel tubes had a 0.77 cm-inside-diameter and a wall thickness of 0.09 cm for the first 28 cm in length which was reduced to an inside diameter of 0.56 cm and a wall thickness of 0.036 cm for the final 2.5 cm in length. Total blockage of the fuel injector plane was constant at 72 percent for both fuel injectors. The fuel was mixed with air in the 20.4-cm-long premixing zone which contained a single thermocouple located approximately 0.4 cm from the wall to detect flashback or autoignition. The catalytic reactor was composed of six, 12-cm-diameter, 2.54-cm-long elements. Catalytic reactor element descriptions are provided in tables I(a) and (b) for the catalytic reactor used with each gasifier. All elements contained a noble metal as the catalyst which was applied to identical substrates. Each element was separated by a 0.32 cm gap which contained at least one thermocouple as shown in Fig. 1. Downstream of the catalytic reactor were four thermocouple planes and a water-cooled, fixed-position, gas-sampling probe with a 0.37 cm inside diameter sampling passage located at the duct centerline. Samples flowed through heated sample lines to continuous gas analyzers. Samples were analyzed for CO, $CO_2$, $NO_x$, unburned hydrocarbons, and $O_2$. Water was injected downstream of the reactor to quench the combustion products before passage through a back pressure valve.

### Westinghouse Fluidized-Bed Gasification System

A schematic drawing of the Westinghouse fluidized-bed coal gasification system is shown in Fig. 3. The gasifier was a single-stage, fluidized-bed unit which operated at a pressure of $16.5 \times 10^5$ Pa. It was operated in both an oxygen-blown and an oxygen-enriched air-blown mode to produce medium, 9.7 MJ/m$^3$ (260 Btu/scf), and low, 5.9 MJ/m$^3$ (160 Btu/scf), heating-value gas, respectively. The product gas cleanup system included a refractory lined cyclone and a quench scrubber to remove most of the particulate matter. The scrubber also removed most of the ammonia and cyanide compounds. Sulfur compounds were not removed. Average product gas compositions are contained in tables II(a) and (b). A more complete description of the Westinghouse fluidized-bed coal gasification system can be found in (10) and (12).

### General Electric Fixed-Bed Gasification System

A schematic diagram of the General Electric fixed-bed gasification system is shown in Fig. 4(a). The gasifier was a fixed-bed reactor which operated at a pressure of $20 \times 10^5$ Pa. It was operated in an air-blown mode to produce low, 3.66 MJ/m$^3$ (98 Btu/scf), heating-value gas. The gasification system also included a complete product gas cleanup system. A schematic of the low-heating-value gas cleanup system is shown in Fig. 4(b). Average gas composition is contained in table III. Sulfur compounds were removed by the cleanup system but ammonia levels were quite high because of the final saturation stage. A more complete description of the General Electric Gasification System can be found in (11).

## MEASURMENTS AND COMPUTATIONS

### Reference Velocity

The reference velocity was computed from the measured air and fuel mass flow rates, the mixture inlet temperature, the duct cross-sectional area, and the test section inlet pressure. The fuel was included because of the relatively large flow rates necessary for the coal-derived gases.

### Emission Index

Emissions were measured as concentrations in ppm by volume, corrected for water of combustion and converted to emission indices as described in (10,11).

### Combustion Efficiency

Combustion efficiency was calculated from the expression:

$$Eff = 100 - \frac{HV_{CH_4}}{HV_{fuel}} \frac{E.I._{HC}}{10} - \frac{HV_{CO}}{HV_{fuel}} \frac{E.I._{CO}}{10}$$

where

Eff = combustion efficiency, %
$E.I._x$ = emission index of specie x, gx/kg fuel
HVx = lower heating value of x, J/kg

Equilibrium concentrations of unburned hydrocarbons and CO were extremely small for the test conditions of this study and were therefore neglected in the calculation of combustion efficiency. It was also assumed that hydrogen would quickly react and not contribute to combustion inefficiency.

### Adiabatic Reaction Temperature

The adiabatic reaction temperature was computed using the computer program of (13) at the inlet mixture temperature, pressure and carbon balance fuel-air ratio. The fuel composition utilized was that reported in tables II and III.

## RESULTS AND DISCUSSION

### Combustion Efficiency

Combustion efficiency data are presented in Figs. 5(a) to (d), for the catalytic reactors operated on low-heating-value gas produced from both gasifiers and medium-heating-value gas produced from the fluidized-bed gasifier. Combustion efficiency is presented as a function of the adiabatic reaction temperature. In Fig. 5(a), combustion efficiency is

shown for the catalytic reactor operated on the low-heating-value gas from the General Electric fixed-bed gasifier. Results are presented for inlet mixture temperatures from 500 to 700 K, reference velocities of 10 and 20 m/s, and pressures of $5x10^5$ and $10x10^5$ Pa. At a reference velocity of 20 m/s, combustion efficiency was increased at an inlet temperature of 700 K compared to 500 or 600 K. Little difference in combustion efficiency is shown for inlet temperatures of 500 and 600 K. As expected, decreasing the reference velocity from 20 to 10 m/s increased combustion efficiency at an inlet temperature of 500 K. Little effect of pressure is shown for the catalytic reactor operated on the of $5x10^5$ and $10x10^5$ Pa. At adiabatic reaction temperatures above 1350 K, combustion efficiencies of 99.5 percent and above were measured for the test conditions shown.

Figure 5(b) presents combustion efficiency data obtained with the low-heating-value gas from the Westinghouse fluidized-bed gasifier. Data are presented at inlet temperatures from 525 to 650 K. As expected, combustion efficiency was generally increased with increasing inlet temperatures except for the 525 K inlet temperature data. These data were obtained before the higher inlet temperature data. The catalytic reactor operated on the coal-derived gas from the Westinghouse fluidized-bed gasifier showed a decline in performance with increasing run time. Inspection of the catalytic reactor after testing revealed a coating of iron oxide on all catalytic reactor surfaces which was probably responsible for the performance decline. Combustion efficiencies of 99.5 percent and above were still obtained at adiabatic reaction temperatures above 1350 K.

In Fig. 5(c), combustion efficiency data are presented for the catalytic reactor operated on medium-heating-value gas produced from the Westinghouse fluidized-bed gasifier. At a reference velocity of 20 m/s, data at an inlet temperature of 525 K show considerably poorer combustion efficiency than higher inlet temperatures. Lower inlet temperatures would be expected to reduce combustion efficiency. However, the data at 525 K were also taken after the higher inlet temperature data, and the catalytic reactor degradation, previously discussed, was probably also responsible for the decline. For combustion efficiencies above 99.5 percent, adiabatic reaction temperatures above 1415 K are required for the test conditions shown in Fig. 5(c).

Combustion efficiency data for all fuels are presented in Fig. 5(d) at a nominal inlet temperature of 600 K, a reference velocity of 20 m/s, and pressures of $5x10^5$ and $10x10^5$ Pa. Combustion efficiency for both low-heating-value gases showed good agreement. The fairly high water content of the General Electric low-heating-value gas, 33 percent, apparently acted only as a diluent. The medium-heating-value gas showed slightly poorer combustion efficiency than either of the low-heating-value gases. Since the catalytic reactor was operated on medium-heating-value gas from the fluidized-bed gasifier after completion of the low-heating-value gas tests, catalytic reactor degradation with run time could have been the cause. Reference 9 reported an effect of H2/CO ratio on combustion efficiency with an increasing H2/CO ratio increasing combustion efficiency. For the present study, the H2/CO ratio was 0.57 for the medium-heating-value gas and 0.61 for the low-heating-value gas from the Westinghouse fluidized-bed gasifier and 1.11 for the low-heating-value gas from the General Electric fixed-bed gasifier. Little effect of H2/CO ratio from 0.57 to 1.1. is apparent from the results of the present study.

Flashback problems were reported in (8,9), which necessitated the use of a flashback arrestor upstream of the catalytic reactor. Flashback tendency was reported in (9) to increase with increasing inlet temperature and decreasing reference velocity. It was also reported to be more severe with medium-heating-value gas than with low-heating-value gas. In the present study, flashback was not a significant problem. No flashback arrestor was utilized and the most severe operating condition, an inlet temperature of 725 K, a pressure of $10x10^5$ Pa, and a reference velocity of 10 m/s using medium-heating-value gas, was run without any indication of flashback.

## CO Emissions

CO emissions, in units of gCO/kg fuel, are presented in Figs. 6(a) to (d) as a function of the adiabatic reaction temperature. In Fig. 6(a), CO emissions are presented for low-heating-value gas produced from the General Electric fixed-bed gasifier. The CO emissions generally show the expected trends. CO emissions were decreased with increasing inlet temperature and decreasing reference velocity. No effect of pressure is shown for pressures of $5x10^5$ and $10x10^5$ Pa.

Figure 6(b) presents data obtained from low-heating-value gas produced from the Westinghouse fluidized-bed gasifier. Little effect of inlet temperature, reference velocity, or pressure is shown for the range of conditions listed. CO emissions decreased rapidly at adiabatic reaction temperatures above 1300 K.

CO emissions from the medium-heating-value gas from the Westinghouse fluidized-bed gasifier are presented in Fig. 6(c). CO emissions were substantially increased for an inlet temperature of 525 K which was probably caused by the lower inlet temperature and catalytic reactor degradation.

Results from all gases at a nominal inlet temperature of 600 K, a reference velocity of 20 m/s, and pressures of $5x10^5$ and $10x10^5$ Pa are presented in Fig. 6(d). CO emissions with low-heating-value gas from the Westinghouse fluidized-bed gasifier were lower than the medium-heating-value gas from the same gasifier and the low-heating-value gas from the fixed-bed gasifier. CO emissions from the medium-heating-value gas were higher than those from both low-heating-value gases. No effect of pressure is apparent. Both low-heating-value gases show similar combustion efficiencies because the CO contribution to combustion inefficiency was relatively small.

## Unburned Hydrocarbon Emissions

Unburned hdyrocarbon emissions in units of $gCH_4/kg$ fuel are presented in Figs. 7(a) to (d) as a function of the adiabatic reaction temperature. Figure 7(a) presents unburned hydrocarbons data obtained with the General Electric fixed-bed gasifier low-heating-value gas. The same trends as previously observed for CO emissions are shown. Unburned hydrocarbon emissions were very low at adiabatic reaction temperatures above 1350 K for all test conditions, as shown in Fig. 7(a).

Figure 7(b) presents unburned hydrocarbon emissions data obtained with low-heating-value gas produced from the Westinghouse fluidized-bed gasifier. The unburned hydrocarbon show the expected trends with inlet temperature and reference velocity

even though the CO emissions from this low-heating-value gas did not.

Unburned hydrocarbon emissions from the Westinghouse fluidized-bed gasifier are shown in Fig. 7(c).

Figure 7(d) presents unburned hydrocarbon emissions for all three gases at a nominal inlet temperature of 600 K, a reference velocity of 20 m/s, and pressures of $5 \times 10^5$ and $10 \times 10^5$ Pa. Unburned hydrocarbons emissions from both low-heating-value gases were similar and lower than those obtained with the medium-heating-value gas.

NOx Emissions

Oxides of nitrogen, ($NO_x$) emissions, the sum of NO + $NO_2$, are presented in Fig. 8 as an emission index, g $NO_2$/kg fuel, for all three coal-derived gases. Test conditions are a nominal inlet temperature of 600 K, reference velocity of 20 m/s, and pressures of $5 \times 10^5$ and $10 \times 10^5$ Pa. No effect of adiabatic reaction temperature is shown. This implies that all $NO_x$ produced was due to conversion of fuel-bound nitrogen in the fuel. $NO_x$ emissions from the fluidized-bed gasifier were about an order of magnitude lower than those from the fixed-bed gasifier. This was caused by the fairly large ammonia content of the fixed-bed gasifier low-heating-value gas. The ammonia content was approximately 3500 ppm by volume and was due to the final gas saturation stage in the product gas cleanup system. Using the approximate value of 3500 ppm, conversion of ammonia in the fixed-bed low-heating-value gas to $NO_x$ was 47 percent. Using the average ammonia concentration from table II for the fluidized-bed gasifier gave ammonia conversion rates to $NO_x$ of 100 percent. It should be mentioned, however, that the ammonia concentrations were subject to considerable variations and the average value given is probably not very accurate.

SUMMARY OF RESULTS

This paper has summarized the more important results for catalytic combustion of actual gasifier produced low- and medium-heating-value gas. Both low, 5.96 MJ/m$^3$ (160 Btu/scf), and medium, 9.7 MJ/m$^3$ (260 Btu/scf), heating-value gas were produced from a fluidized-bed gasifier at Walz Mill, Pennsylvania, operated by Westinghouse. Low-heating value gas, 3.65 MJ/m$^3$ (98 Btu/scf), was produced from a fixed-bed gasifier at Schenectady, New York, operated by General Electric. Essentially identical test hardware and catalytic reactors were supplied by NASA Lewis to the contractors for experimental testing at their respective gasifier sites.

Combustion efficiencies greater than 99 percent were obtained for all three coal-derived gaseous fuels. For the fluidized-bed gasifier, $NO_x$ emission ranged from 0.2 to 0.4 g $NO_2$/kg fuel for both the low- and medium-heating-value gases. $NO_x$ emissions from the fixed-bed gasifier with low-heating-value gas were considerably higher and ranged from about 2.0 to 4.0 g $NO_2$/kg fuel. The increase in $NO_x$ emissions was caused by the increased fuel-bound nitrogen content ($NH_3$) of the fixed-bed gasifier low-heating-value gas, which was estimated at 3500 ppm by volume. Flashback from the catalytic reactor into the premixing zone upstream was not a severe problem and only occurred a few times for each fuel. Test conditions of inlet mixture temperatures up to 700 K, pressures up to $10 \times 10^5$ Pa, and reference velocities as low as 10 m/s were investigated without flashback occurring.

Some catalytic reactor performance degradation was apparent with the fluidized-bed gasifier produced gas. Posttest inspection revealed an iron oxide coating on all catalytic reactor surfaces which was probably responsible for the degradation. Both catalytic reactors were damaged during the experimental testing. Cracked and melted portions of the reactor elements were found at the conclusion of the testing. Test conditions were rather severe for the fairly low melting temperature catalytic reactor substrate. The studies were not intended to demonstrate long term durability or damage-free operation but to perform parametric studies at combustor conditions representative of stationary gas turbines.

REFERENCES

1. Anderson, D. N., "Performance and Emissions of a Catalytic Reactor with Propane, Diesel, and Jet-A Fuels," NASA TM-73786, 1977.
2. Pfefferle, W. C., et. al., "Catathermal Combustion; A New Process for Low Emissions Fuel Combustion," ASME Paper 75-WA/FU-1, 1975.
3. Rosfjord, T. J., "Catalytic Combustion with Incompletely Vaporized Residual Fuel," UTRC-R81-914/24-18, United Technologies Research Center, East Hartford, Conn., Mar. 1981. (NASA CR-165161)
4. Dodds, W. J., and Ekstedt, E. E., "Demonstration of Catalytic Combustion with Residual Fuel," R81AEG590, General Electric Co., Cincinnati, OH., Aug. 1981. (NASA CR-165369)
5. Bulzan, D. L., and Tacina, R. R., "Catalytic Combustion of Residual Fuels," NASA TM-82731, 1981.
6. Chu, E. K., Snow, G. C., and Tong, H., "Catalytic Combustion of Coal-Derived Liquid Fuels," EPRI AP-1666, Acurex Corp., Mountain View, CA., Jan. 1981.
7. Bulzan, D. L., and Tacina, R. R., "Catalytic Combustion of the Coal-Derived Liquids," NASA TM-81594, 1981.
8. Lee, H. C. and Osgerby, I. T., "Catalytic Combustion Characteristics of Low- and Medium BTU Gas Fuels," Fourth Workshop on Catalytic Combustion, EPA-600/9-80-035, pp. 457-489.
9. Osgerby, I. T., "Catalytically Supported Thermal Combustion of Coal Derived Low-Btu Gas, Parts 1 and 2," Report No. FE/2683, Engelhard Minerals and Chemical Corp., Edison, N.J., 1981.
10. Schwab, J. A., "Low- and Medium-Heating-Value Coal Gas Catalytic Combustor Characterization," Westinghouse Electric Corp., Madison, PA, 1981. (NASA CR-165560)
11. Blanton, J. C. and Shisler, R. A., "Evaluation of Catalytic Combustion of Actual Coal-Derived Gas," SRD-82-023, General Electric Corp., Schenectady, NY, 1982. (NASA CR 167842)
12. Salvador, L., et. al., "The Westinghouse Coal Gasification Process," International Gas Research Conference, Government Institutes, 1980.
13. Gordon, S. and McBride, B. J., "Computer Program for Calculation of Complex Chemical Equilibrium Compositions, Rocket Performance, Incident and Reflected Shocks and Chapman-Jouguet Detonations," NASA SP-273, 1976.

TABLE I. - CATALYTIC REACTOR ELEMENT DESCRIPTIONS

(ELEMENTS NUMBERED FROM INLET)

(a) Westinghouse Fluidized-Bed Gasifier Catalytic Reactor, Low- and Medium-Heating-Value Gas

| Element | Catalyst | Loading, $Kg/m^3$ | Substrate | Cell density $cells/cm^2$ | Open area, percent |
|---|---|---|---|---|---|
| 1 | Pt | 5.3 | Corning Cordierite | 46.5 | 63 |
| 2 | Pd | 5.3 | ↓ | ↓ | ↓ |
| 3 | Pd | 5.3 | | | |
| 4 | Pd | 3.6 | | | |
| 5 | 2 Pd/1 Pt | 3.6 | | | |
| 6 | 2 Pd/1 Pt | 3.6 | | | |

(b) General Electric Fixed-Bed Gasifier Catalytic Reactor, Low-Heating-Value Gas

| | | | | | |
|---|---|---|---|---|---|
| 1 | 2 Pd/1 Pt | 1.8 | Corning Cordierite | 46.5 | 63 |
| 2 | ↓ | 1.8 | ↓ | ↓ | ↓ |
| 3 | | 1.8 | | | |
| 4 | | 3.6 | | | |
| 5 | | 3.6 | | | |
| 6 | | 3.6 | | | |

TABLE II - AVERAGE GAS COMPOSITION,

WESTINGHOUSE FLUIDIZED-BED

GASIFIER

(a) Low-heating-value gas

| Component | Volume, percent |
|---|---|
| $H_2$ | 17.23 |
| CO | 28.31 |
| $CH_4$ | 2.29 |
| $CO_2$ | 22.13 |
| $N_2$ | 29.59 |
| $H_2S$ | .14 |
| $NH_3$ | .0135 |

(b) Medium-heating-value gas

| | |
|---|---|
| $H_2$ | 25.22 |
| CO | 44.06 |
| $CH_4$ | 4.47 |
| $CO_2$ | 25.55 |
| $N_2$ | .50 |
| $H_2S$ | .20 |
| $NH_3$ | .0135 |

TABLE III. - AVERAGE GAS COMPOSITION,

GENERAL ELECTRIC FIXED-BED GASIFIER,

LOW-HEATING-VALUE GAS

| Component | Volume, percent |
|---|---|
| $H_2$ | 14.3 |
| CO | 12.9 |
| $CH_4$ | 3.1 |
| $CO_2$ | 5.4 |
| $N_2$ | 30.9 |
| $H_2O$ | 33.4 |
| $NH_3$ | .35 |

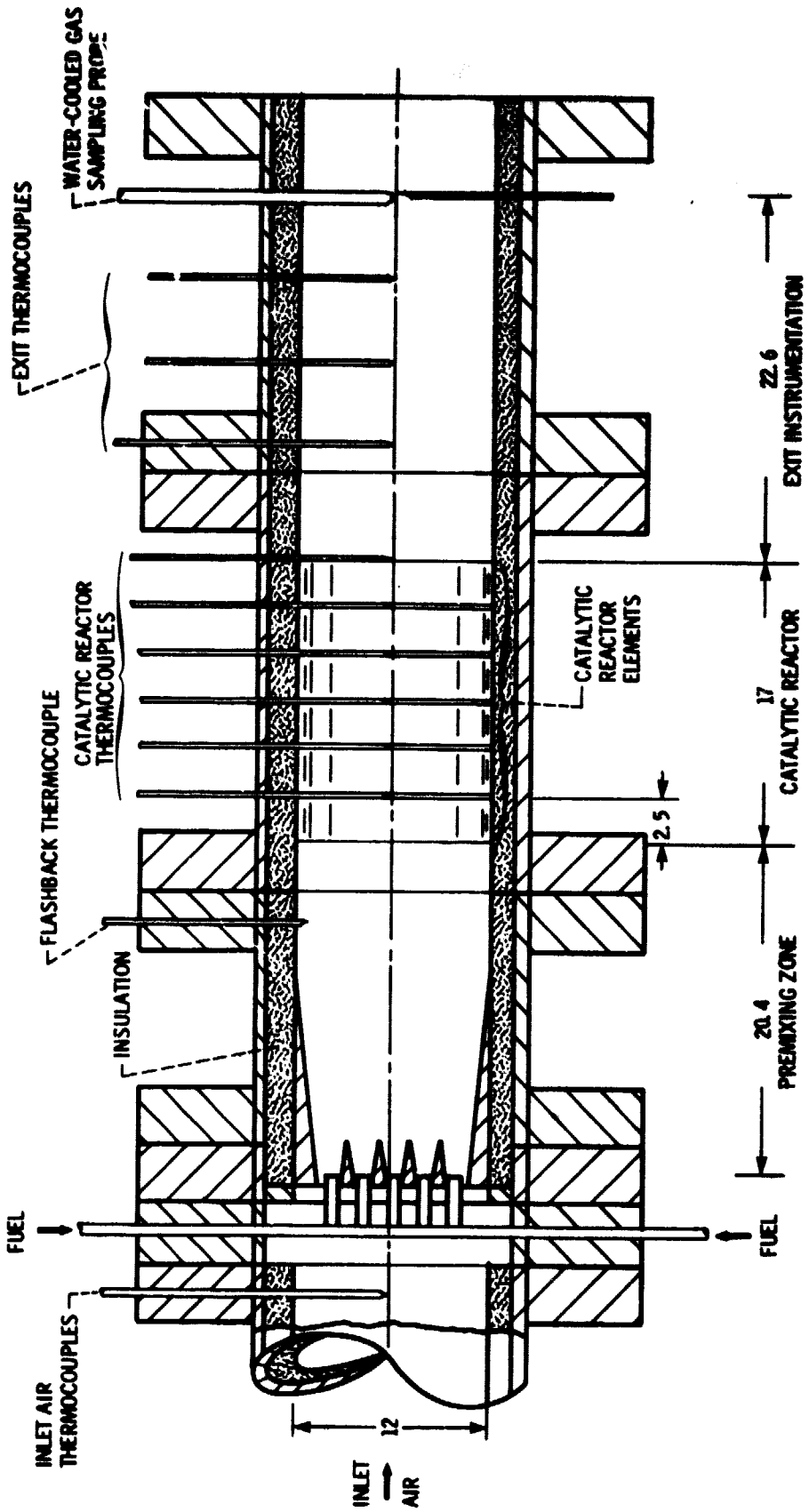


Figure 1. - Test rig schematic.

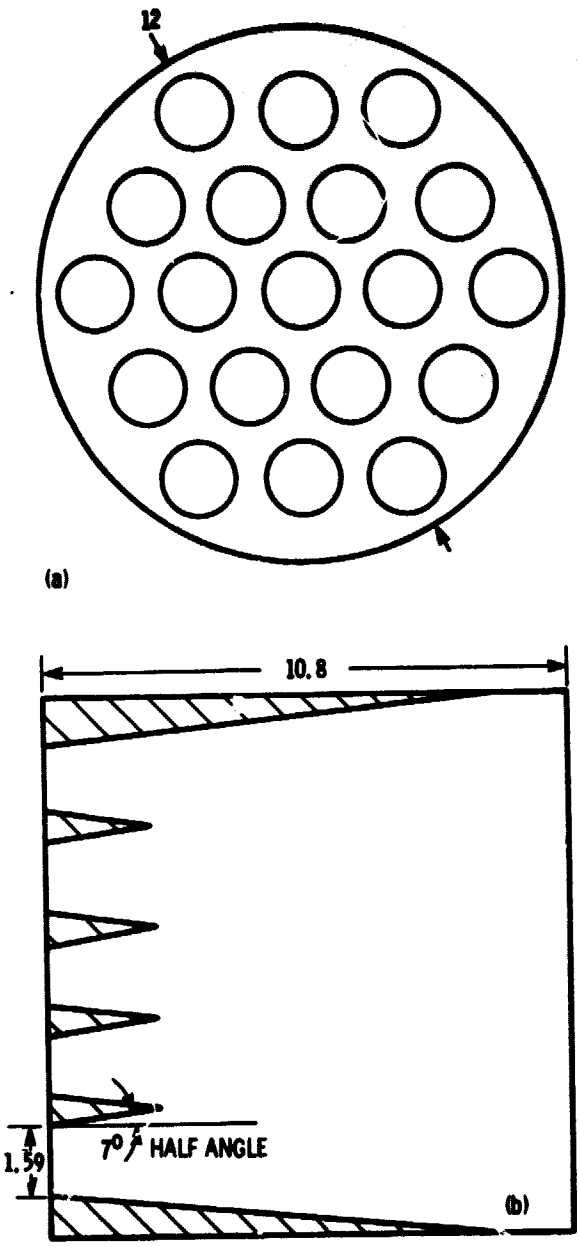


(a) Base, front view, looking downstream.
(b) Base, side view.

DIMENSIONS IN cm

Figure 2. - Fuel injector.

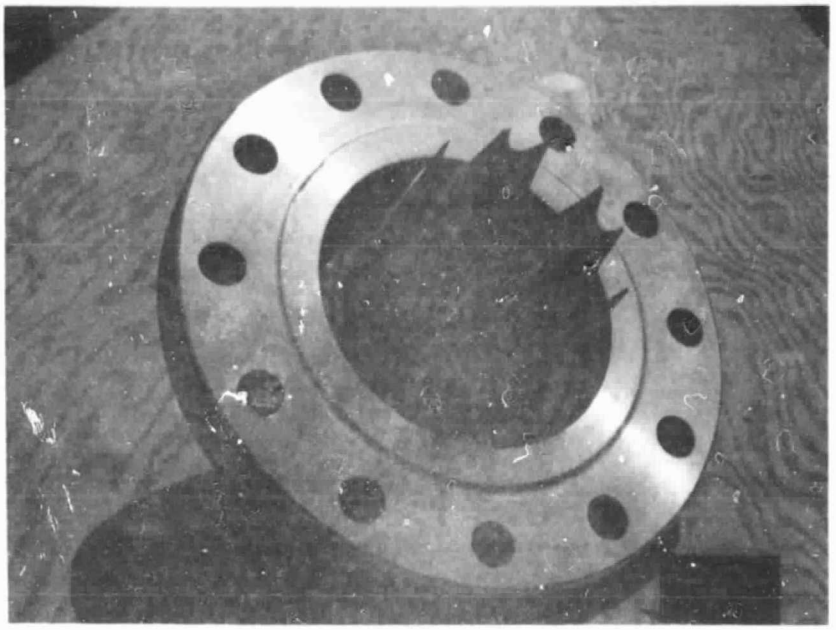

(c) Base photograph, looking upstream.

Figure 2. - Continued.

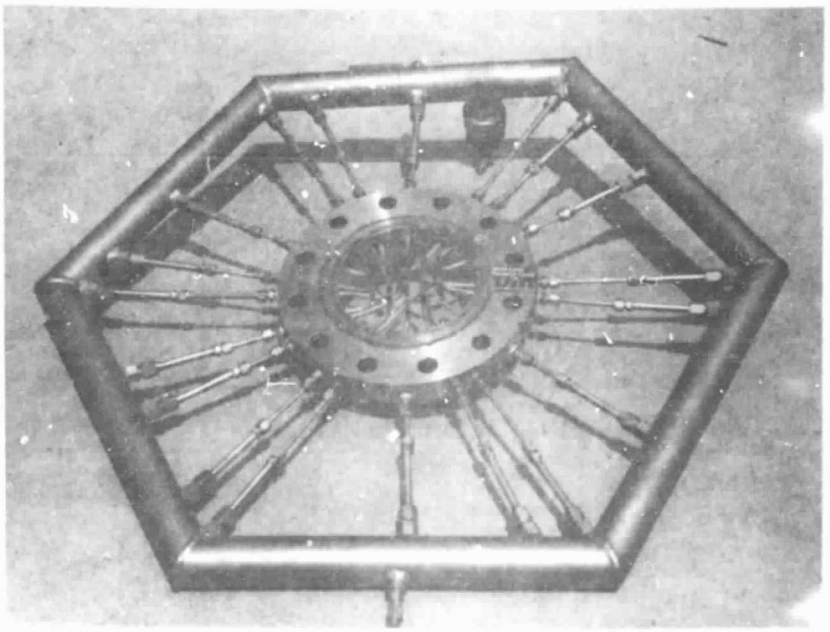

(d) Tube assembly, looking upstream.

Figure 2. - Concluded.

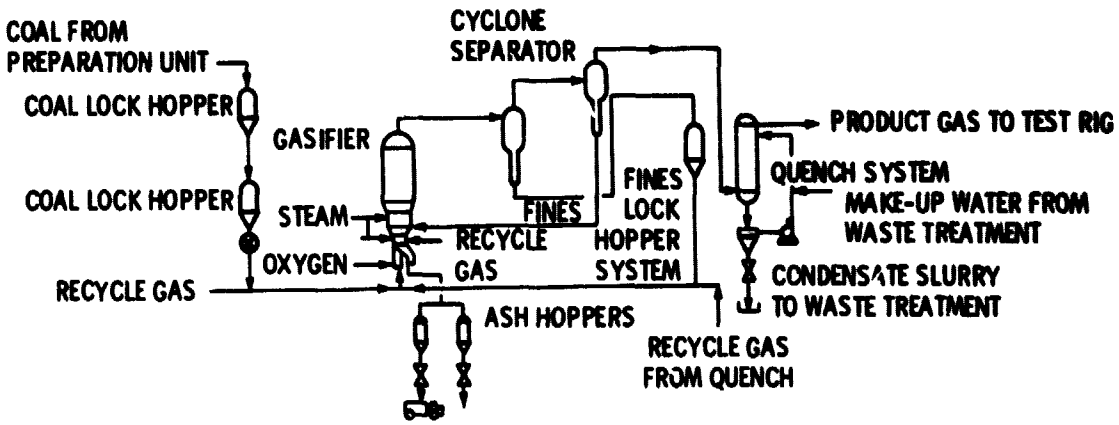


Figure 3. - Westinghouse fluidized bed gasifier system schematic.

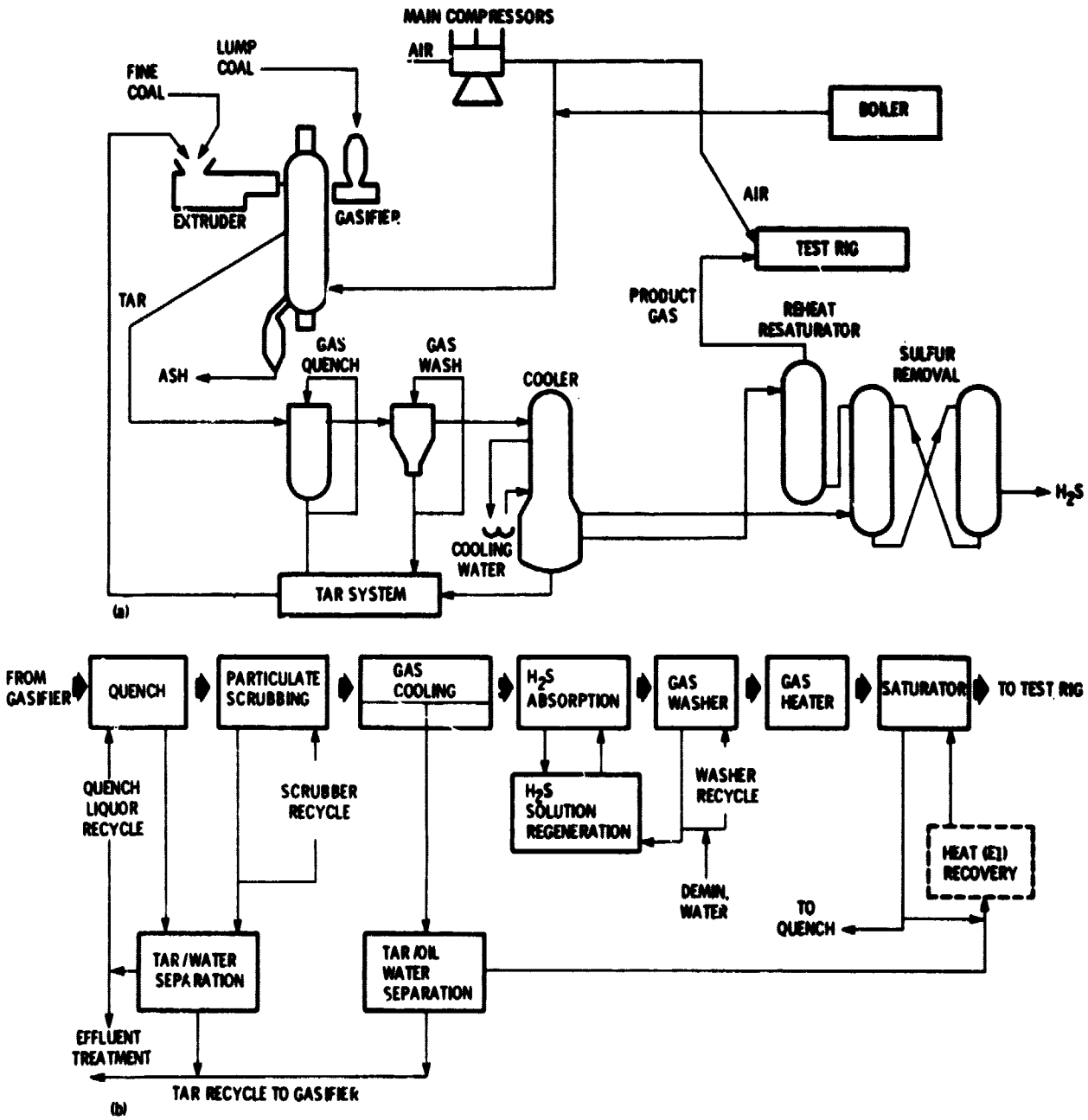


(a) Schematic diagram of General Electric fixed-bed gasifier and product gas cleanup system.

(b) Low-heating valve gas cleanup system.

Figure 4. - General Electric fixed-bed gasifier and low-heating valve gas cleanup system schematic.

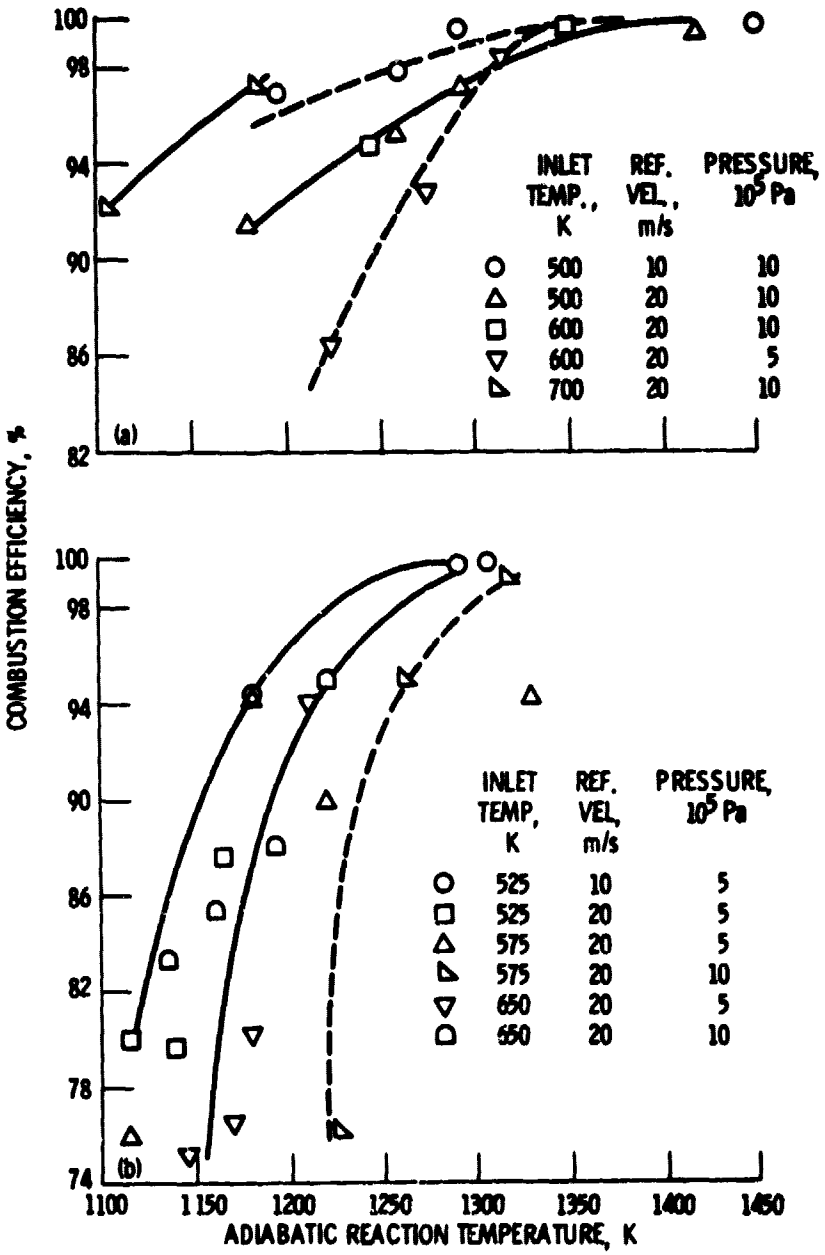


(a) General Electric fixed-bed gasifier, low-heating value gas.
(b) Westinghouse fluidized-bed gasifier, low-heating value gas.

Figure 5. - Combustion efficiency.

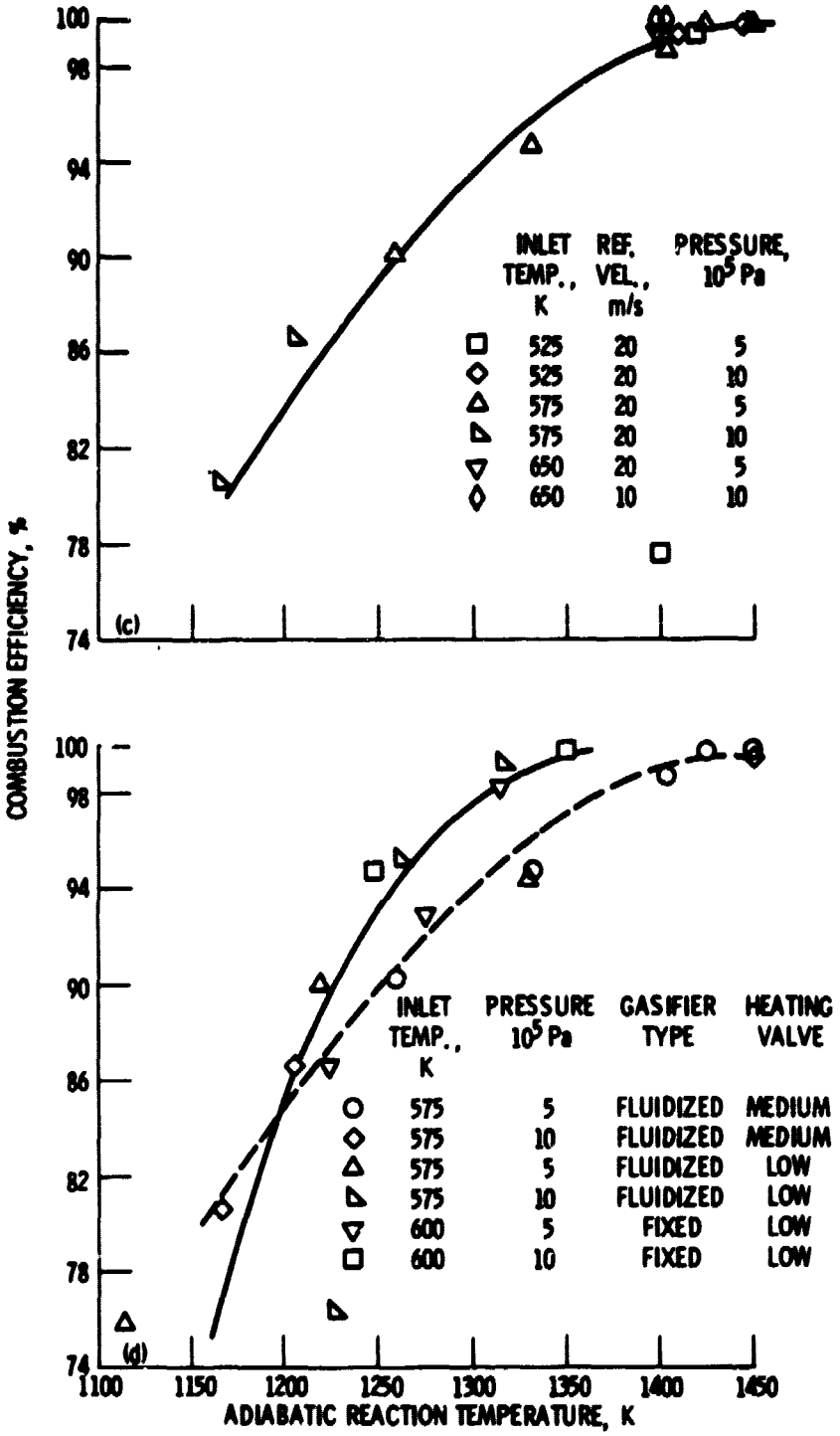


(c) Westinghouse fluidized-bed gasifier, medium-heating valve gas.

(d) All gases; reference velocity, 20 m/s.

Figure 5. - Concluded.

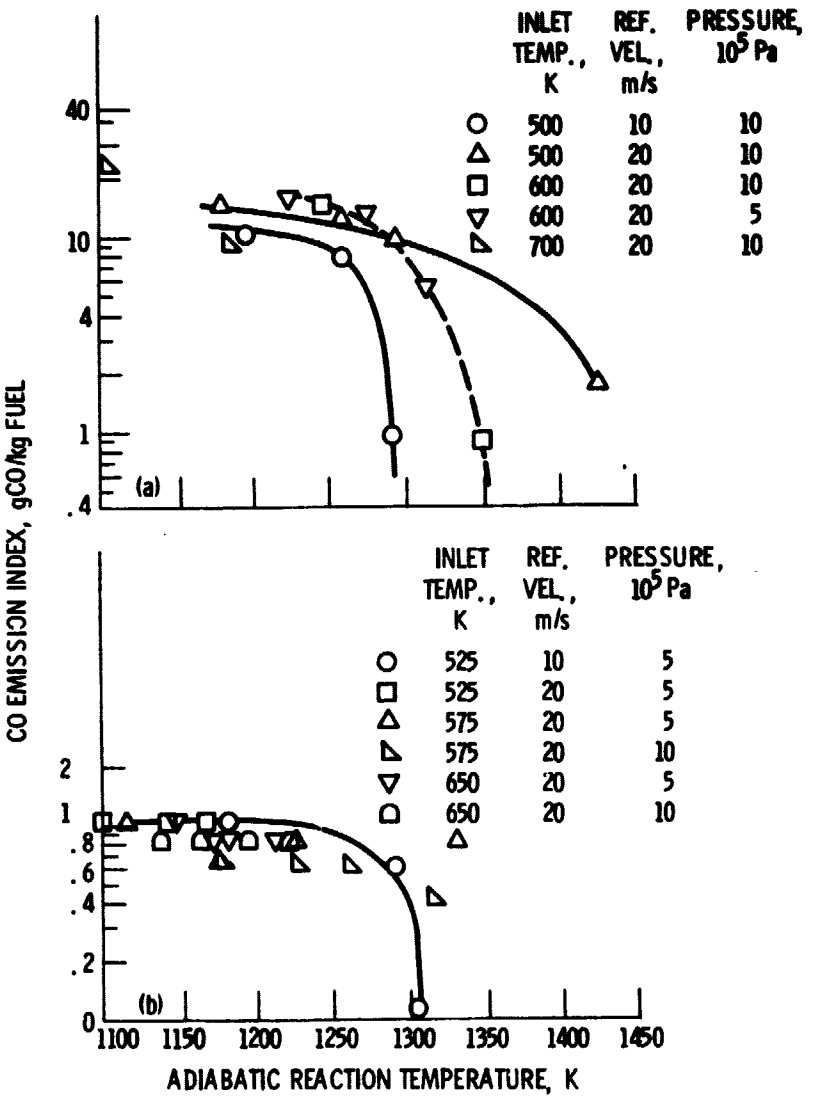


(a) General Electric fixed-bed gasifier, low-heating valve gas.

(b) Westinghouse fluidized-bed gasifier, low-heating valve gas.

Figure 6. - CO emissions.

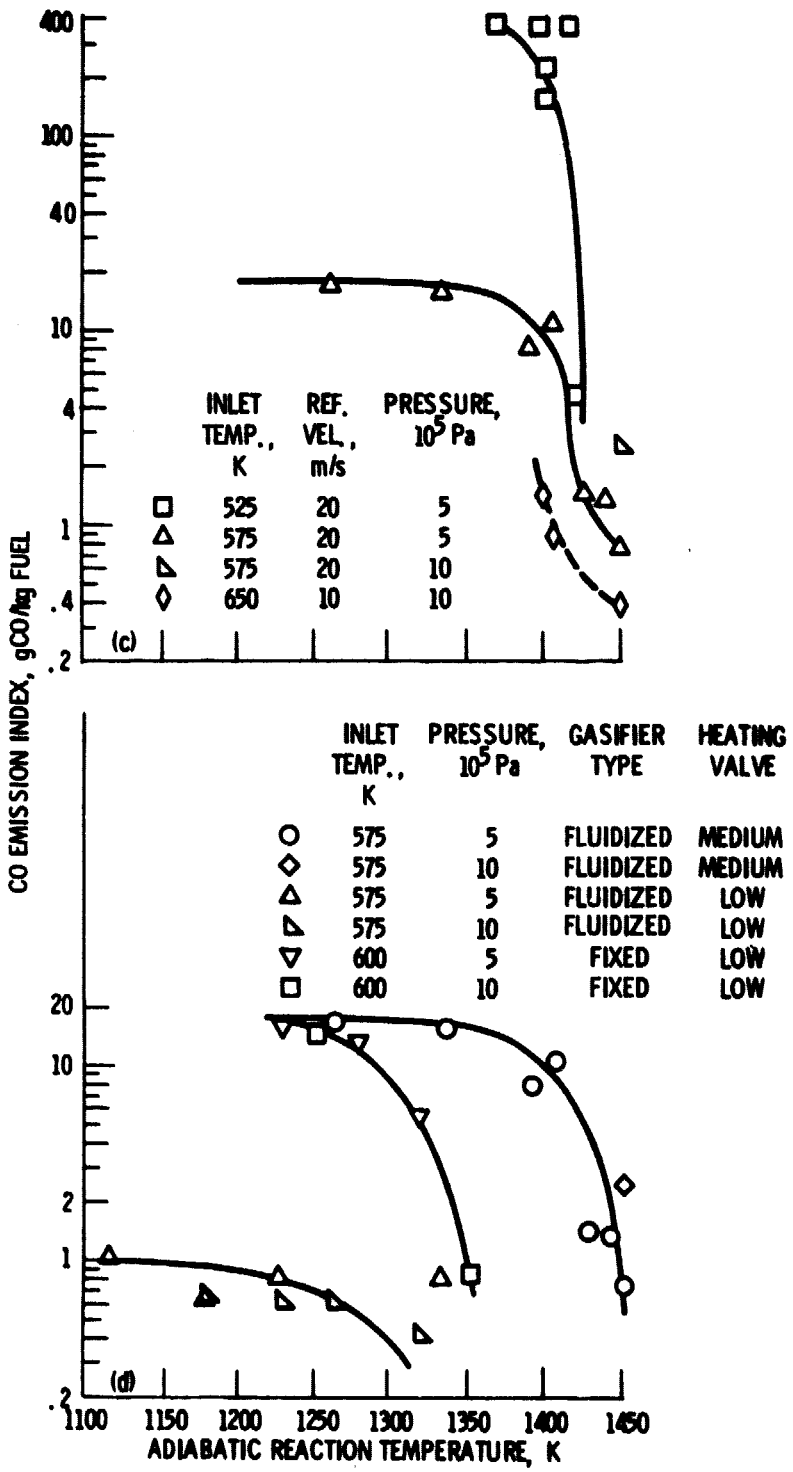


(c) Westinghouse fluidized-bed gasifier, medium-heating valve gas.

(d) All gases, reference velocity, 20 m/s.

Figure 6. - Concluded.

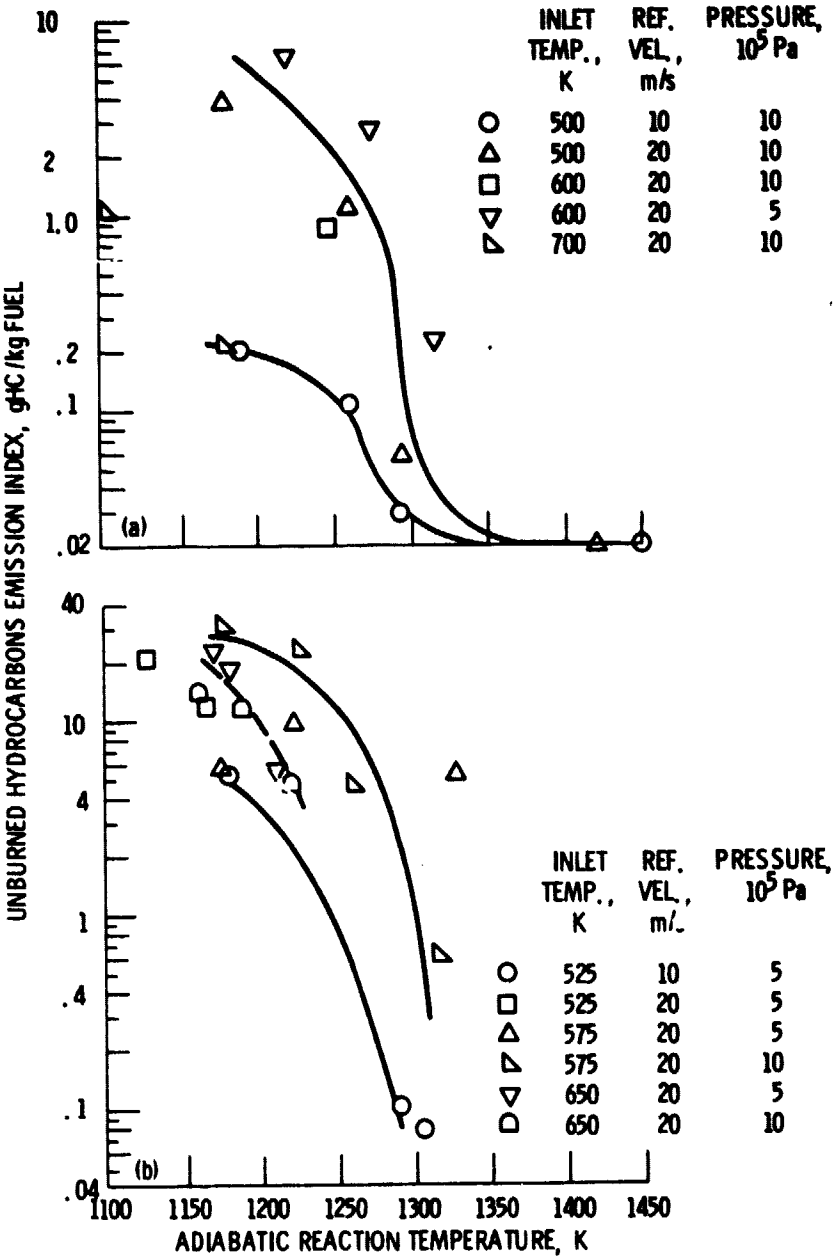


(a) General Electric fixed-bed gasifier, low-heating valve gas.

(b) Westinghouse fluidized-bed gasifier, low-heating valve gas.

Figure 7. - Unburned hydrocarbon emissions.

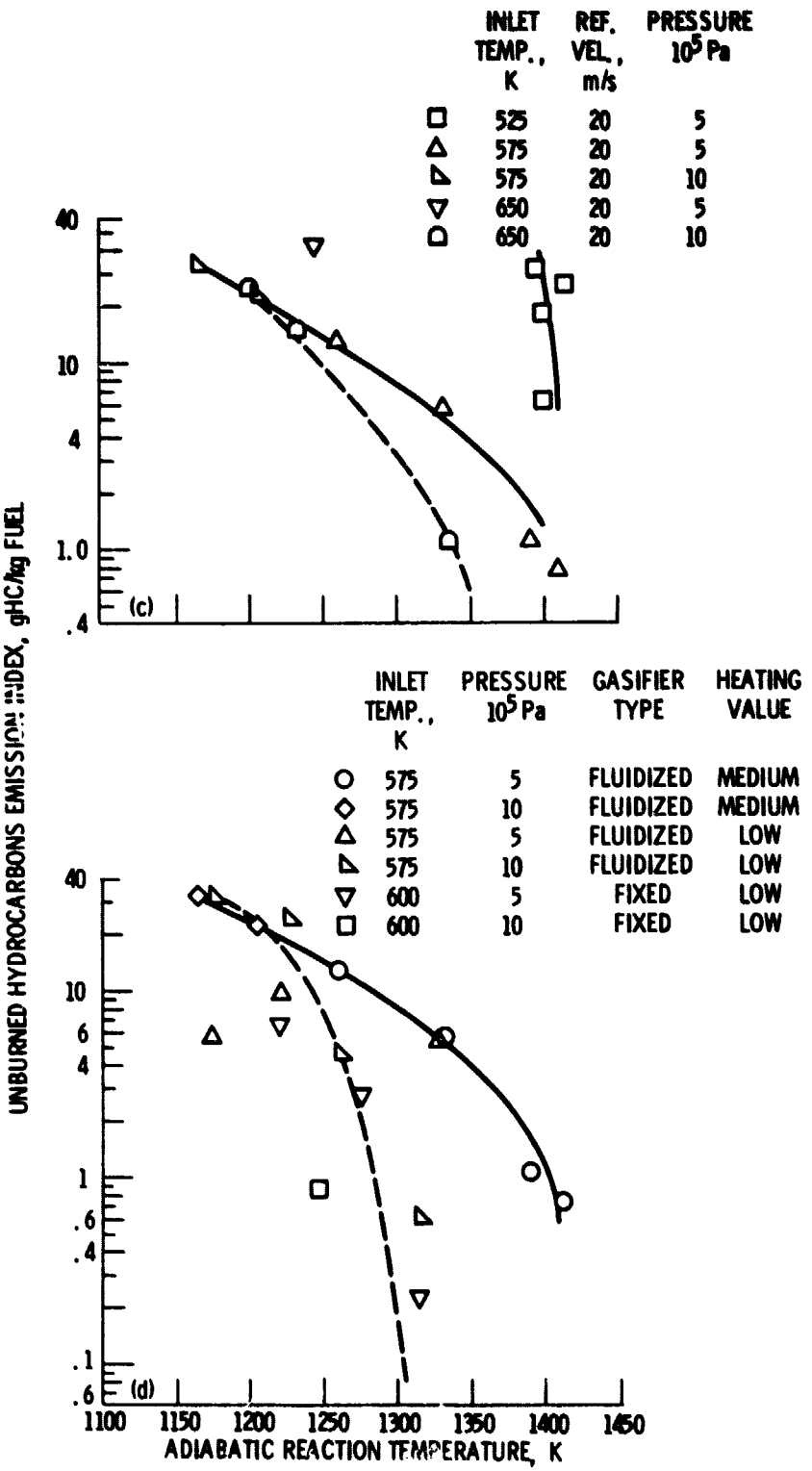


(c) Westinghouse fluidized-bed gasifier, medium-heating valve gas.

(d) All gases; reference velocity, 20 m/s.

Figure 7. - Concluded.

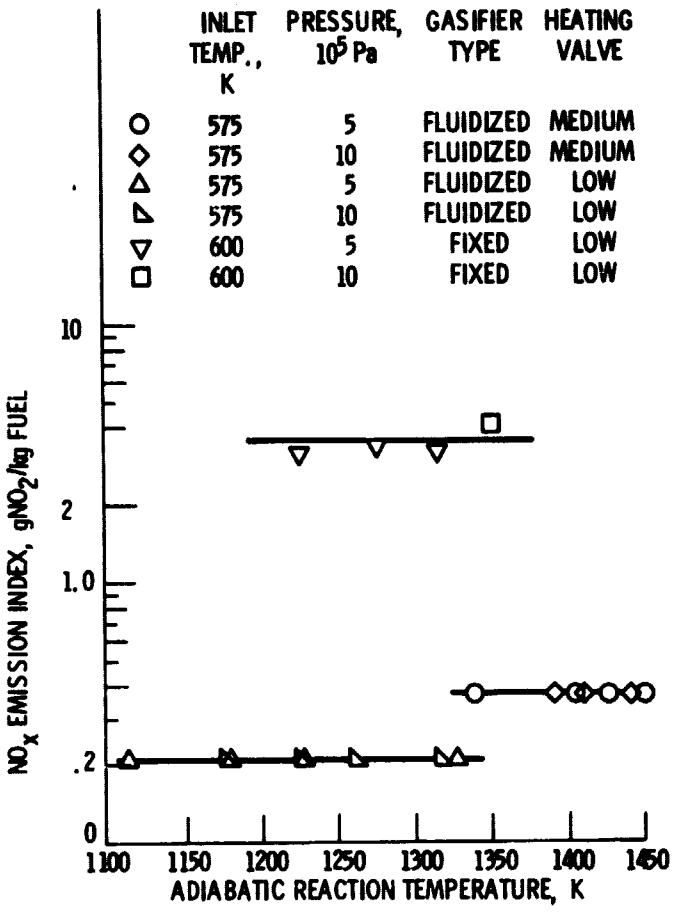


Figure 8. - $NO_x$ emissions; all gases; reference velocity, 20 m/s.